POLITECNICO DI TORINO
Repository ISTITUZIONALE

Influence of liquid-binder ratio on the performance of alkali-activated slag mortar with superabsorbent polymer

(Article begins on next page)

25 April 2024

Influence of liquid-binder ratio on the performance of alkali-activated slag mortar with superabsorbent polymer

Zhengxian Yang [a], Peng Shi [a,b], Yong Zhang [a], Zhenming Li [c,*]

[a] *College of Civil Engineering, Fuzhou University, Fuzhou, 350108, China*
[b] *Department of Structural, Geotechnical and Building Engineering, Politecnico di Torino, Turin, Italy*
[c] *Department of Materials and Environment (Microlab), Faculty of Civil Engineering and Geoscience, Delft University of Technology, Delft, the Netherlands*

ARTICLE INFO

ABSTRACT

The influences of liquid-binder ratio and mixing sequence on the performance of superabsorbent polymer (SAP)-containing alkali-activated slag (AAS) mortar are investigated in this study. It is found that the SAP absorbs much less liquid in upper supernatant of AAS than in water. Mixing SAP with liquid first induces a larger absorption capacity of the SAP than mixing it with solid first. Increasing the liquid-binder ratio improves the flowability but reduces the strength of AAS mortar with SAP. Nonetheless, the strength of internally cured mixtures is higher than that of the reference even with an extra liquid-binder ratio of 0.09. The reason behind lies in the refinement of capillary and gel porosity by internal curing, despite the presence of large voids originated from SAP. The autogenous shrinkage of AAS paste is reduced significantly by the incorporation of SAP but the further mitigating effect of increased liquid-binder ratio is limited.

1. Introduction

In recent years, the growth of construction industries leads to a vigorous development of concrete manufacturing [1]. Due to the low cost and stable performance, ordinary Portland cement (OPC) has become an indispensable construction material [2]. However, the high consumptions of cement bring a severely negative impact on the environment [3,4]. To release the pressure of environmental pollution, alkali-activated materials (AAMs) have gradually attracted more attention in the favor of low CO_2 emission compared with OPC. AAMs could present superior mechanical properties, desirable workability and satisfactory durability [5–8]. However, the practical application of AAMs is still limited, one reason for which lies in their large shrinkage that may induce micro or macro cracking [9–12].

Tailoring the curing regime could be an effective method to mitigate the shrinkage of concrete [13]. As an important part of the concrete production, curing is vital and is generally divided into external curing and internal curing as shown in Fig. 1. External curing provides extra moisture for concrete by means of spraying water in the construction site. External curing is common in practice, but only has a significant curing effect on the surface, and mainly helps to prevent plastic cracks due to evaporation [14]. In comparison, internal curing is realized by pre-introducing water-absorbing materials into the concrete [15]. It has been known that the hydration of binder results in a decrease of internal relative humidity (RH), which causes capillary pore pressure and eventually leads to autogenous shrinkage [16]. Internal curing agents can act as local "water reservoirs" [17], which release the pre-absorbed water to compensate the

---

water consumption, so that the internal RH of the concrete can be maintained and the self-desiccation-induced shrinkage can be mitigated.

Superabsorbent polymer (SAP) is one commonly used internal curing agent in concrete. SAP is rich in hydrophilic groups, such as -COOH and -OH. Before SAP absorbs water, the polymer chains are intertwined forming a three-dimensional network [17,18]. Once the SAP contacts with water, the hydrophilic groups will be ionized, resulting in ion concentration difference between the inside and outside of the SAP and causing osmotic pressure. Thus, water is continuously absorbed into SAP until achieving saturation in the form of hydrogel. The water absorption capacity of SAP in tap water (or distilled water) can reach hundreds or even thousands of times its own weight [19]. Even in the pore solution of alkali activator, the absorption capacity can still reach dozens of the weight of SAP [20].

SAP has been found to improve many properties of concrete [21]. It can effectively reduce the autogenous shrinkage and consequent cracking, improve the freeze-thaw resistance and promote self-healing of OPC or AAMs systems [18,20,22–24]. Besides, the incorporation of SAP also influences the workability of concrete. Snoeck [25] et al. reported that the incorporation of 0.4% SAP was equivalent to a decrease of 0.05 w/c. In order to ensure a constant slump of concrete, extra water was needed in the mixture. Alternatively, Craeye [26] et al. found that adding pre-saturated SAP can increase the amount of free water and improve the workability of concrete. However, the compressive strength of the concrete can be reduced due to the extra water introduced by SAP [27]. There seems a dilemma between workability and mechanical properties when choosing the water-cement ratio of the system. Given a low water-cement ratio, the incorporation of SAP can promote further hydration of cement and improve the degree of hydration so that the strength can be improved [28,29], but when the initial water content is too high, the extra liquid introduced by SAP will leave big voids as defects that harm the mechanical properties of the matrix [30,31].

While many studies have dealt with the influence of liquid-binder ratio on the properties of SAP-containing cementitious materials, related studies on AAMs are very rare. Song [32] et al., Li et al. [20,33] and Tu et al. [18] all studied the influence of different contents of SAP on the internal RH and shrinkage of slag/fly ash based AAMs, but the content of additional liquid used in these studies were all pre-designed according to the results from either tea-bag method or flowability tests, and were increased proportionally with the SAP dosage. In those cases, there are two variables in the design, SAP contents and liquid-binder ratio, the effects of which are always coupled. Moreover, in paste or mortar, SAP particles pre-mixed with solids may not absorb as much as measured in bulk liquid, e.g., in tea-bags, due to the competition with solid precursors in absorbing liquid during mixing. In addition, slag based AAMs normally show fast setting, before which the maximum absorption capacity of SAP may not be reached yet [34]. Hence, the pre-designed contents of additional liquid in these studies may not be the same as really absorbed by the SAP during casting. In particular, when the SAP dosage varies, the liquid absorption in the system also varies. In another word, the basic liquid-binder ratio of the matrix studied in these researches was not controlled. These issues make it hard or even impossible to draw conclusions on the influences of single factor, e.g. liquid-binder ratio, on the properties of AAMs.

To this end, the goal of this study is set to investigate the influence of liquid-binder ratio on the properties of SAP-containing alkali-activated slag (AAS) with the content of SAP fixed at various mixing conditions. The SAP is introduced by pre-mixing with either solid (dry mixing) or liquid (wet mixing). The workability, mechanical properties, autogenous shrinkage and pore structure of the AAS mortars are experimentally studied and influence of liquid-binder ratio is clarified.

2. Principle of internal curing and absorptivity

The internal RH of the binder decreases gradually due to external environmental factors e.g. drying, and hydration process. As a small local liquid 'reservoir', the absorbent material releases the pre-absorbed water stored due to humidity gradient and negative pressure in capillary pores, which keeps a dynamic balance of the internal RH of mortar or concrete structure without external water supplement. As a result, the hydration can be enhanced and the structure can be denser. When the surface tension of concrete pores changes, the vapor pressure of pore water will also change, and the change of vapor pressure is related to the migration and loss of water during curing [35], which is characterized by Laplace formula (Eqn 1):
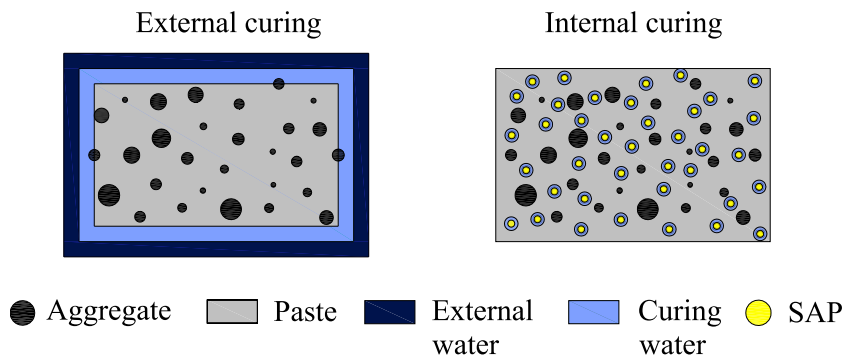
$$P_s - P_w = \frac{2\sigma \cos \theta}{r} \tag{1}$$

Fig. 1. Comparison of internal and external curing of concrete.

where σ is water/vapor interfacial tension, $N \cdot m^{-1}$; θ is moist angle, °; P_s is water vapor pressure, Pa; P_w is water pressure, Pa; and r is the radius of the crescent-shaped hole , *mm*.

In a specified unsaturated state, there will be a critical pore size, below which the pores are saturated. Water in the macropores will migrate and transport to the micropores [36]. For internal curing materials, their pore sizes are normally larger than that of the capillary pores of the paste, so the stored water in the absorbent material will gradually migrate to the surrounding paste.

The biggest difference between SAP and other internal curing materials like light-weight aggregate is that SAP has fast water absorption, high absorption capacity and good water retention. Because SAP contains hydrophilic groups, when it contacts with water, there will be interaction forces leading to swelling of SAP [37]. When absorbing water, the hydrophilic groups are ionized and the ionized cations can move freely inside the solution, while the anions remain unchanged on the high polymer molecular chain (Fig. 2). With the deepening degree of ionization, the amount of anions on the polymer chain gradually increases, which causes the repulsion between the ions and the expansion of SAP. Then, the internal cation concentration becomes increasingly higher, resulting in the ion concentration difference within the structure, which further strengthens the liquid absorption capacity of SAP. When the ion gradient and intermolecular force maintain a dynamic equilibrium, the absorbent polymer reaches a saturated state and the liquid will be released when a new relative humidity gradient forms, so as to provide internal curing.

3. Experimental

3.1. Materials and mix proportion

3.1.1. Materials

Ground granulated blast-furnace slag (GGBFS) was provided by Shanxi Longze Water Purification Materials Co., Lt. The slag had a specific surface area of 1.31 m^2/g and a density of 2.91 g/cm^3. The chemical composition of slag is shown in Table 1. The X-ray diffraction (XRD) of slag is shown in Fig. 3 (a). The slag contained a large amount of amorphous phase while some crystals were also detected, such as calcite and quartz. The particle size distribution of the slag obtained by laser Particle Size Analyzer is shown in Fig. 3 (b).

The superabsorbent polymer (SAP) used in the study was a self-made polyacrylic acid SAP. The raw materials mainly included acrylic acid, methacrylic acid, acrylamide and hydroxypropyl acrylate. The scanning electron microscope (SEM) image and particle size distribution of the SAP particles are shown in Fig. 4. It can be seen that the SAP had irregular shapes and the particle size of SAP was mainly between 100–1000 μm, much larger than that of slag particles. Table 2 lists the physical parameters of SAP.

A mix of sodium hydroxide (provided by China Pharmaceutical Group), sodium silicate (provided by Shandong Yousuo Chemical Technology Co., Ltd.) and tap water was used as the activator. The sodium silicate (8.3 wt % of Na$_2$O and 26.5 wt % of SiO$_2$) was mixed with deionized water and solid sodium hydroxide (purity ≥96.0%) to obtain the activator. The activator was prepared one day before the casting to ensure an ambient temperature of the solution.

The sand used in the experiment was standard sand provided by Xiamen Aisiou Standard Sand Co., Ltd. The sand belonged to the medium sand in Zone II. Polycarboxylate superplasticizer in the state of light-yellow liquid was used. The superplasticizer was Point-758 supplied by Kezhijie New Materials Group and had a density of 1.04 g/cm^3.

3.1.2. Mix proportion

Table 3 shows the specific information of the AAS mortar mix proportion. The Na$_2$O dosage was 6% by weight of slag and the modulus of the activator is 0.93 (the mass ratio of sodium silicate to sodium hydroxide was 1:0.273). The SAP content was fixed at 0.2% of the mass of slag, which was identified as an optimal dosage according to the results of a previous study [38]. The reference mixture S0 had a water-binder ratio of 0.36 (the binder was considered as the combination of slag and the solid alkalis). Various contents of extra water (0.03, 0.06 and 0.09) were considered to study the influence of liquid content on properties of AAS mortar with SAP. Two mixing ways of SAP, dry mixing (D) and wet mixing (W), were considered by which the SAP was mixed with dry solids or with liquid first before mixing with the other components. The binder-sand ratio was 0.56 for all mixtures. As an example of the terms
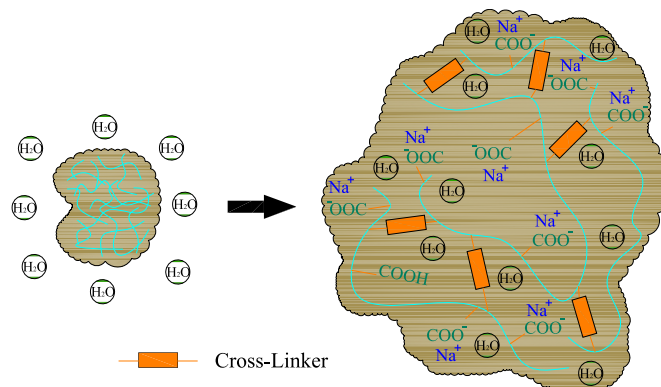

Fig. 2. Changes of structure before and after absorption of the SAP.

Table 1
Chemical compositions of slag (wt.%).

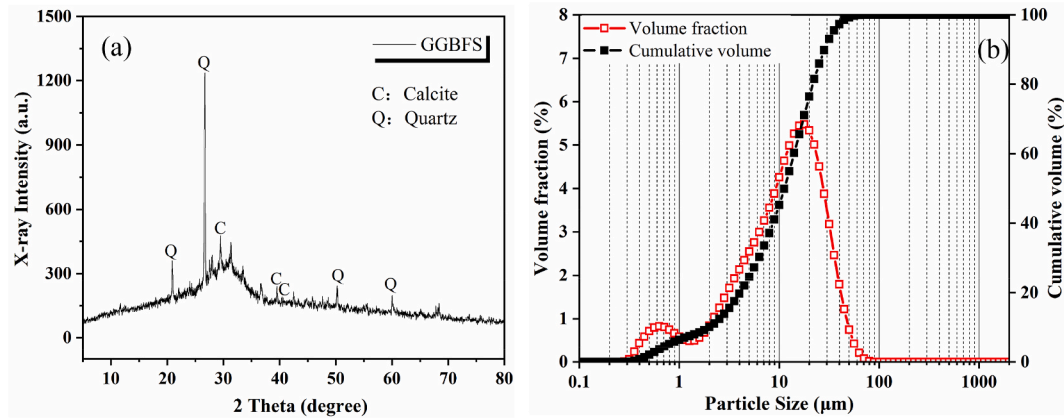| Oxide	CaO	SiO₂	Al₂O₃	Fe₂O₃	MgO	TiO₂	MnO	SO₃	K₂O	P₂O₅	Other	LOI
Slag	47.00	21.90	13.00	0.74	8.07	0.89	0.35	2.50	0.36	0.02	2.91	2.26

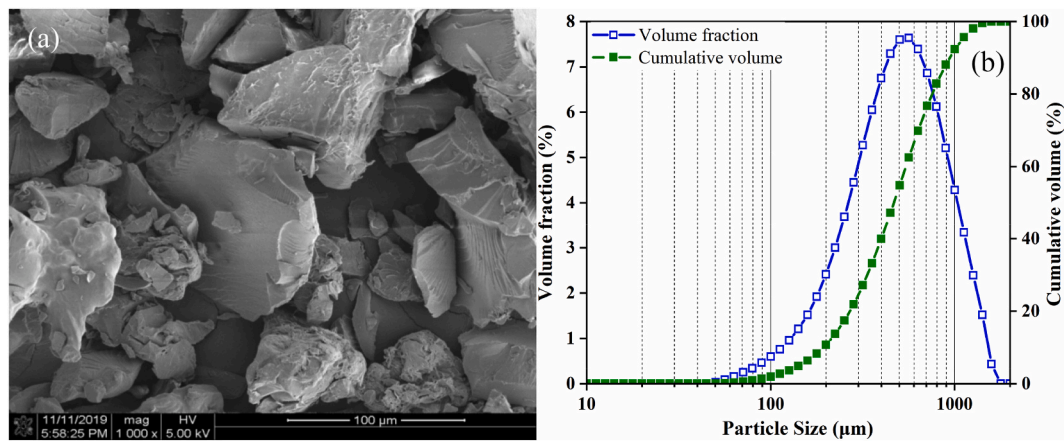**Fig. 3.** XRD pattern (a) and particle size distribution (b) of the slag.

Fig. 4. SEM image (a) and particle size distribution (b) of SAP.

Table 2
Physical properties of SAP.

Moisture content (%)	Bulk density (g/cm³)	Specific surface area (m²/g)	Appearance	Solubility
3.5	0.572	0.015	Fine white powder	Insoluble in water

Table 3
Mix proportion of the specimens.

Code	SAP (kg/m³)	Slag (kg/m³)	Sand (kg/m³)	SiO₂ (kg/m³)	Na₂O (kg/m³)	H₂O (kg/m³)	PCSP (kg/m³)	Water-binder ratio Basis	Water-binder ratio Extra
S0	–	646	1292	35	38.8	258.4	0.646	0.36	–
S0.2D(W)0	1.292	646	1292	35	38.8	258.4	0.646	0.36	–
S0.2D(W)0.03									0.03
S0.2D(W)0.06									0.06
S0.2D(W)0.09									0.09

of different mixtures, S0.2D0.03 means the mortar with a SAP content of 0.2%, added in dry state, and an extra water-binder ratio of 0.03.

3.2. Test methods

3.2.1. Absorptivity of SAP

The absorption capacities of SAP in tap water and upper supernatant of AAS paste was measured by tea-bag method [39,40]. The reason why supernatant of AAS paste was used lies in the intention to mimic the initial pore solution of the paste as much as possible. In a previous study [20], activating solution was directly used in the measurement of absorptivity of SAP. While the activator does contain Na^+, OH^- and SiO_3^{2-}, which distinguish the environment from water, other ions like Ca^{2+} released from the dissolution of slag can also influence the absorption of SAP [41]. Hence, this study used the supernatant of paste rather than the direct activator. The method for obtaining the supernatant of AAS paste was as follows. The mixture was evenly stirred according to the S0 paste ratio. After hardening for 1 day, 10 g sample was put into agate mortar and ground into powder. Then, 500 g deionized water was added and the suspension was placed in an oscillator for 24 h. The supernatant of AAS paste was obtained by slow filtration with qualitative filter paper.

To measure the absorption, a 200 mesh (particle size of 0.074 mm) nylon bag was pre-absorbent and weighed at first. 1 g superabsorbent polymer was weighed and placed at the bottom of each nylon bag. Then, they were placed in tap water or supernatant solution and the containers were sealed with to avoid moisture loss. The mass of the bag with SAP was measured regularly until the mass is stable. Before each weighing, the superabsorbent polymer was placed on a 200 - mesh stainless steel screen, and the excess water was filtered through the filter net. The process was repeated and gently flipped for about 5 min until the quality of the absorbent polymer was not changed. Then the water absorption rate ϖ_i of SAP at different time periods can be calculated by Eqn 2:

$$\varpi_i = \frac{M_i - M_2 - M_1}{M_2} \times \frac{1}{\rho_w} \tag{2}$$

where M_i is the total mass of absorbent polymer and nylon bag at different times, g; M_2 is the mass of the dry powder of absorbent polymer, g; M_1 is the mass of the pre-absorbent nylon bag, g; ρ_w is the density of the solution, g/cm^3.

Two replicates were measured for each solution.

3.2.2. Setting time

Referring to ASTM C191-13 [42], the setting time of the mortar specimens was measured by a Vicat machine. The needle penetrated every 5 min near the initial setting and every 15 min near the final setting.

3.2.3. Flowability test

According to ASTM C1437-01 [43] and GB/T 2419-2005 [44], a NDL-3 mortar Fluidity Tester was used. First, the surface of the jumping table and the inner wall of the test die were cleaned by a damp cloth. Then the mixed mortar was poured into the test die. A tamping bar was used to stamp the mortar for 15 times. After tamping, a small knife was used to remove excess mortar on the surface. The jump table was allowed to vibrate for 25 times. The diameter of the two vertical directions of the spread was measured and the average value was taken.

3.2.4. Compressive strength

The test method of the strength referred to GB/T 17671-1999, using a YAW-300C automatic compressive testing machine. The specimens were put into the standard curing room after demoulding and the strength was measured on 3 days, 7 days, 28 days and 56 days. The temperature in the curing room was maintained at (20 ± 2) °C and the humidity was >98%. 6 specimens were measured for each mixture.

3.2.5. Autogenous shrinkage

A NS-NC-12 Shrinkage Tester was used to test the autogenous shrinkage of AAS paste. Paste instead of mortar samples were used for this test aiming at magnifying the difference in shrinkages of different mixtures. The fresh mixed paste samples were cast into corrugated tubes to measure the free length change [45]. The length of bellows was 420 ± 5 mm, and the outer diameter is 29 ± 0.5 mm. The mold was sealed to prevent water loss during the test, and the samples were kept at constant temperature at 22.0 ± 2.0 °C. The tests started from the final setting time and the data was recorded every minute.

3.2.6. Reaction heat

The reaction heat of the AAS paste was measured via an eight-channel isothermal calorimeter TAM Air for 7 days. The mix proportion of the samples were the same as shown in Table 3 but without sand. The total amount of slag in each channel was 10 g, and other additives varied according to the mix ratio. The paste was stirred evenly and the Abe bottle was put into the instrument for measurement immediately after mixing. The indoor temperature and humidity (about 20.0 ± 0.1 °C and 60 ± 2% RH) were kept constant during the test to avoid disturbance.

3.2.7. Scanning electron microscope

The samples cured for 28 days were put into isopropanol to stop hydration for 7 days and then dried in a vacuum drying oven at 60 °C until constant mass before subject to SEM test. The epoxy resin was pressed into the sample pores through the vacuum pump and kept in vacuum for more than 3 h. When the epoxy was completely condensed and hardened, five grades of sandpapers with different

fineness were used to polish the surface with anhydrous ethanol lubricated. Ultrasonic cleaning was used to remove impurities. Afterwards, 9 μm, 6 μm and 1 μm diamond suspension polishing liquid was uniformly sprayed on the surface of polished surface in turn to further polish the sample. Quanta 250 scanning electron microscope was used for the backscattering electron test of AAS mortar (BSE). The samples need to be sprayed with gold during the test.

3.2.8. Pore size analysis

The sample cured for 28 days was broken into small particles and immersed in isopropanol for 7 days to stop the reaction. The samples were then put in a vacuum drying oven at 60 °C until a constant weight was reached. The intrusion and extrusion mercury test were carried out by PoreMaster-60 automatic Mercury Intrusion Porosimeter to analyze the pore size distribution and porosity of AAS mortar with different additional water-to-binder ratios.

4. Results and discussion

4.1. Water absorption

The absorption capacities of SAP in tap water and AAS paste are shown in Fig. 5. It can be seen that SAP has a far higher absorption capacity in water, 160.7 g/g, compared with the absorption capacity of SAP in the supernatant of AAS paste, 30.8 g/g. Even though the absorption capacity of SAP is different in different aqueous solutions, the adsorption process followed a similar trend.

The reason why the absorption capacity of SAP in the supernatant of AAS is only about 19.2% of that in tap water lies in the ions contained in the supernatant. It has been reported that the water absorption capacity of SAP decreases gradually with the increase of the density of anionic groups in $Ca(OH)_2$ solution [46], and the presence of multi-ions in the solution changes the interaction forces between molecules in SAP polymer chains due to the electronic barrier effect. Especially, Ca^{2+} and Al^{3+} can cause cross-linking of molecular chains [47]. These effects were not considered in previous studies [20]. Moreover, the absorption of SAP also relies on the ion concentration difference between internal and external environments [48]. Since the supernatant has high concentrations of ions, the osmotic pressure would be lower and the absorption capacity of SAP is reduced. The results also verified Jensen's argument [21] that the variety of ions in the cement slurry and the high ion concentrations of the solution are the two main factors that cause the difference in absorption capacity of SAP.

4.2. Setting time

Table 4 shows the initial and final setting time of AAS mortar with different mixing conditions and various water contents. The setting time of S0.2 system is shorter than that of S0, because the SAP absorbs liquid and induces a lower initial interstitial porosity of the matrix. Hence, less time is needed for the initial products to form a network with a certain stiffness. In general, dry mixed samples show longer setting times than wet mixed ones, indicating that the SAP absorbs more in wet condition.

In bulk liquid, the SAP is allowed to absorb liquid freely before contact the solid. Among dry particles, however, the absorption of liquid by SAP is actually under a certain restraint by the viscous slurry, and the wetting of precursor and sand competes with the absorption by SAP. Therefore, the initial absorption capacity of SAP in solid would not be as high as has been absorbed in liquid. Moreover, the dissolution of slag would release more ions, which were not contained in the activator, such as Ca^{2+}, Al^{3+}, etc [49]. The increase of the concentrations of multi-ions can harm the electronic barrier effect in SAP and cause crosslinking of polymer chains as discussed in Section 3.1 [47,50]. These effects will hamper the further absorption of liquid in SAP. As a result, both the absorption rate and capacity in SAP in dry-mixed mixtures are limited so that more liquid is present in the interatrial space and a longer setting time is shown.

When extra liquid is added, the setting time of the mortar increases. There are two main reasons for this. First, extra liquid is present
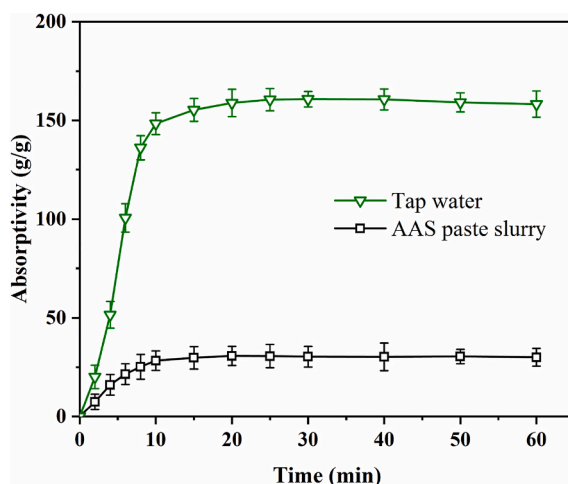

Fig. 5. SAP absorptivity with time in tap water and supernatant of AAS paste.

Table 4
Setting time of AAS mortar under different mixing condition.

Setting time (min)	S0	S0.2_0		S0.2_0.03		S0.2_0.06		S0.2_0.09	
		D	W	D	W	D	W	D	W
Initial	28	16	12	24	19	30	26	42	35
Final	55	40	35	50	43	66	52	74	65

so that a higher basic liquid-binder ratio is produced in the matrix which means a larger initial porosity. Furthermore, a higher water content in the activator results in lower concentrations of ions which are essential to the dissolution of slag and formation of initial reaction products. Therefore, too high extra liquid-binder ratio, e.g., 0.09, induces a longer setting time than that of the reference.

4.3. Flowability

The flowability results are shown in Fig. 6. Compared with the reference group, the flowability of S0.2D0 and S0.2W0 decreased by 15% and 22%, respectively. By introducing extra water, the flowability is improved. It is found that the wet mixing process causes a poorer flowability than the dry mixing, but the difference between the two decreases with the increase of additional water-binder ratio. When the extra water-binder ratio increases to 0.09, the difference is only 5 mm.

SAP can absorb liquid in the activator and reduce the actual liquid-binder ratio of the mortar, thus a lower flowability is expected if no extra water is introduced. The two mixing sequences result in different flowability of the mortar, which can be explained by the larger absorption capacity of SAP in liquid, as discussed in the previous section. When the liquid content is increased, these effects would be relieved, so the difference in the absorption capacities between dry mixed samples and wet mixed samples become smaller.

4.4. Compressive strength

The compressive strength of all AAS mortar samples increased with curing ages. The incorporation of SAP without extra liquid improves significantly the compressive strength, especially at the early age. The 3 days compressive strength of both S0.2D and S0.2W is above 60 MPa, which is even higher than the compressive strength of S0 at 7 days. With the increase of liquid-binder ratio, the compressive strength of SAP-containing AAS mortar becomes lower regardless of the mixing sequence. Despite, the compressive strength of these samples is still higher than the AAS mortar without SAP in all the ages studied. This indicates that the incorporation of SAP in AAS systems does not necessarily reduce the strength while maintaining a comparable workability [32]. The higher compressive strength of SAP-containing samples than S0 is actually the result of coupled effects of SAP incorporation: introduction of big voids on one hand, and reduction of local liquid-binder ratio and porosity in vicinity on the other hand, given a reasonable extra water-binder ratio (this point will be verified in Section 4.7 and 4.8). The results in this section shows that the first effect not always overwhelms.

In previous studies [20,33], strength loss was observed for SAP-containing mixtures, which was probably due to excessive additional liquid. In those studies, the content of additional liquid content was designed according to the absorption capacity of SAP in bulk liquid, which should be higher than the realistic absorptivity in solid precursors, as discussed in Section 4.2. The results in previous studies and this study indicate that the strength of SAP-containing AAS actually depends on the liquid/binder ratio and also the mixing way. Compared with dry mixing, wet mixing induced lower compressive strength in all ages. This is probably because of the larger and even connected voids introduced by wet SAP, which was not as evenly dispersed as by dry mixing. This point will be verified in Section 4.7 by SEM.
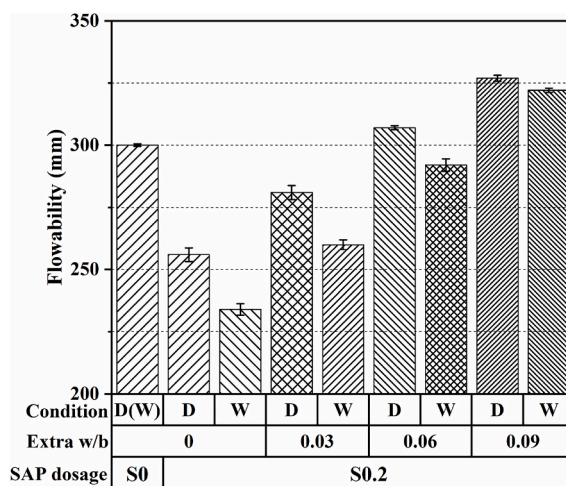

Fig. 6. Flowability of AAS mortar with SAP with different liquid-binder ratios.

4.5. Autogenous shrinkage

The autogenous shrinkage of the paste mixtures is shown in Fig. 8. It can be seen that the addition of SAP can dramatically reduce the autogenous shrinkage of AAS paste, regardless of the liquid content. This is because of the internal curing effect of SAP, which can effectively mitigate the self-desiccation, although it may not be the exclusive mechanism of the autogenous shrinkage of AAS [23]. All SAP-containing mixtures show less than half of the autogenous shrinkage of the reference mixture. Increasing the liquid content can further reduce the autogenous shrinkage, but the effect is not as significant as made by the presence or absence of SAP. This is consistent with the findings of Li et al. [20]. Compared with dry mixing, wet mixing of SAP induces slightly lower autogenous shrinkage due to the larger absorption capacity of SAP in bulk liquid and the consequent higher extent of internal curing.

From the autogenous shrinkage point of view, it seems higher liquid-binder ratio is beneficial for SAP-containing mixtures, however, too high liquid contents are not recommended due to their effect in reducing the compressive strength. Considering all the parameters discussed in the above sections, it seems the optimal extra liquid-binder ratio for AAS mortar with 0.2% addition of SAP is 0.06, which leads to a comparable workability, improved strength and reduced autogenous shrinkage. A higher SAP content will require a higher extra liquid content in order to realize a comparable workability. The microstructure of the SAP-containing samples will be discussed in following sections to explain the macro-scale properties.

4.6. Reaction heat

The reaction heat flow and cumulative heat results of AAS paste under different mixing conditions are shown in Fig. 9. It can be seen that compared with the S0 group, AAS pastes with SAP show lower main reaction peak, regardless of the mixing procedure. With more liquid introduced, the main reaction peak is delayed and becomes lower but broader (Fig. 9 (a) and (c)). This is consistent with the findings of Li et al. [20]. The reasons behind lie in the buffering effect of SAP, which gradually releases activator during acceleration period and dilutes the pore solution containing ions released from slag. Eventually, however, the stored liquid will participate into the reactions so that the reaction degree of the paste in longer-term could be enhanced. As shown in Fig. 9 (b) and (d), the total reaction heat of mixtures with SAP was lower than that of S0 in the first days due to the reduced main reaction peak, but tends to exceed that of S0 in a longer term as indicated by the slope of the curves, especially for the ones with more liquid. Compared with dry mixing, wet mixing induces more apparent changes in the heat flow in acceleration and deceleration period, probably due to the larger amount of liquid absorbed by SAP in this way, as already discussed in previous sections. In both mixing ways, the mixtures with an extra w/b of 0.09 release the highest reaction heat.

4.7. BSE analysis

The BSE images of AAS mortar cured for 28 days is shown in Fig. 10. The phases identified by different gray values in the images from bright to dark are unreacted slag, reaction produces, sand, cracks and pores. The brightness of products and sand is similar, but sand has big particle size, which distinguished it from products surrounding unreacted slag particles. Some microcracks are found in the images, which might be the result of shrinkage occurred during curing or sample preparation [51]. The reference mixture S0 shows few capillary pores in the matrix, indicating a dense pore structure of the material, as consistent with the results of Li et al. [33]. The main reason for the dense microstructure of AAS mortar lies in the fact that the activator provides not only a high pH environment for the dissolution of slag, but also nuclei (e.g. silicates) for the growth of reaction products in the interstitial space [52].

Big black pores present in SAP-containing samples as a result of the water desorption of SAP. Comparing Fig. 10 (b) and (d), or (c) and (e), it can be seen that increasing the liquid-binder ratio induces big pores in the matrix, indicating that more liquid is absorbed by the SAP. These pores act as defects, which harm the strength of the mixture. This is one reason why higher liquid-binder ratio samples have lower compressive strength (Fig. 7). Comparing Fig. 10 (b) and (c), or (d) and (e), it is seen that wet mixed samples show bigger pores than dry mixed samples when the liquid-binder ratio is the same. This verifies the hypothesis that wet mixing enables larger absorption of SAP particles, which can provide enhanced internal curing. However, the big pores in, e.g., S0.2W0.03, are close or even
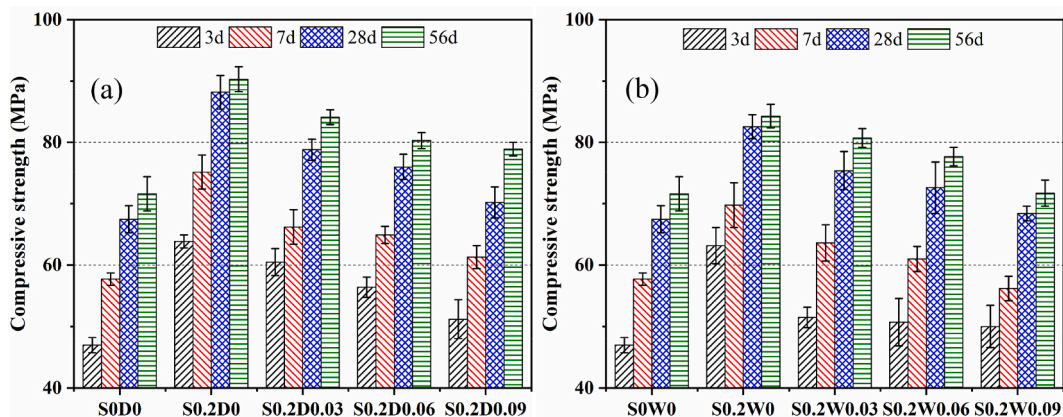
Fig. 7. Compressive strength of AAS mortar with SAP with different liquid-binder ratios: (a) dry mixing, (b) wet mixing.
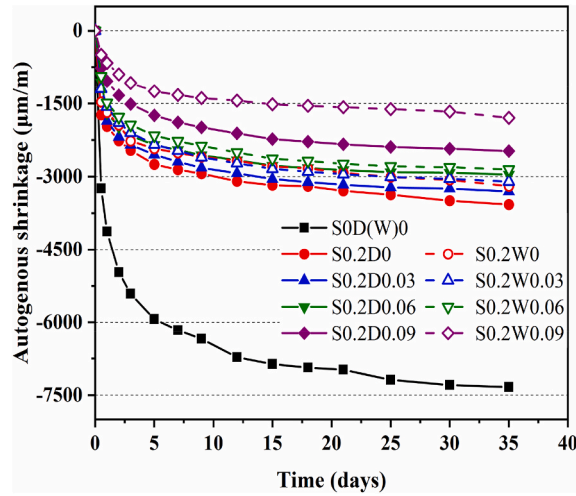
Fig. 8. Autogenous shrinkage of AAS mortar with SAP with different liquid-binder ratios.
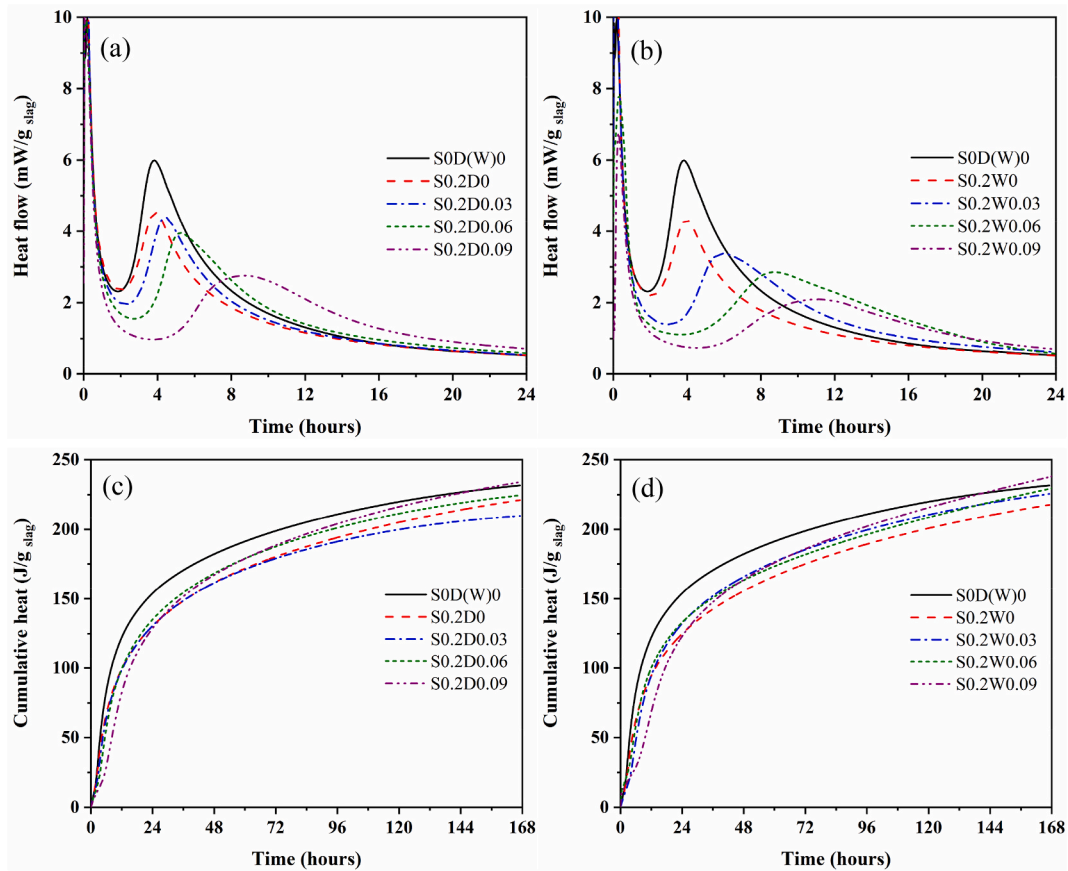

Fig. 9. Reaction heat flow and cumulative heat of AAS paste with different liquid-binder ratios. (a) and (b): dry mixing, (c) and (d) wet mixing.

connected to each other rather than evenly distributed in the matrix, indicating that wet mixing may not be favorable from the SAP dispersion point of view. As shown in Fig. 8, the shrinkage-mitigating effect of SAP in wet mixed AAS mortar is not much evident than that in dry mixed sample. The unevenly distributed SAP particles should be one reason for that, since the liquid desorption will be heterogeneous too, making the internal curing to the matrix insufficient.
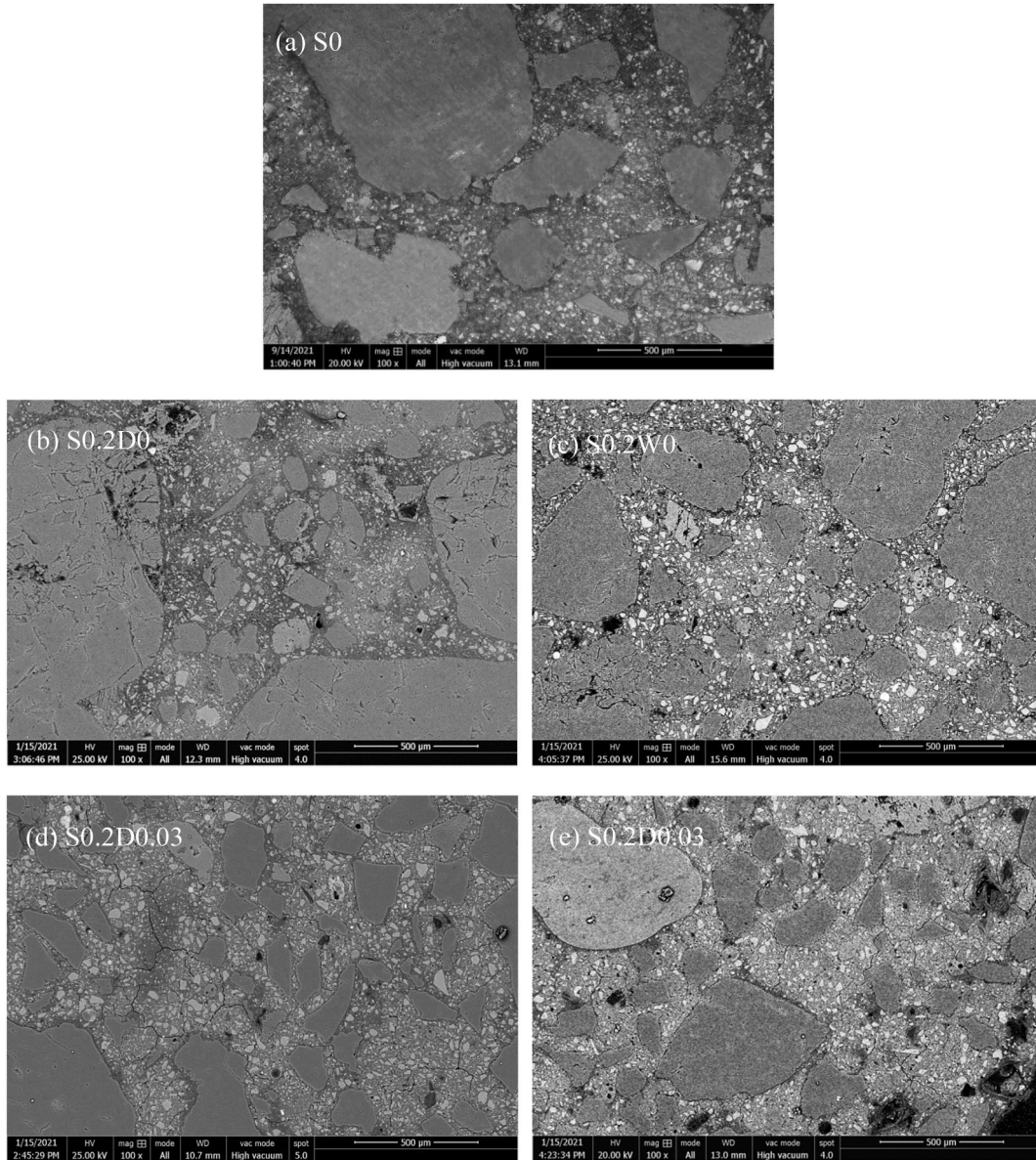
Fig. 10. BSE images of AAS mortar with SAP with different liquid-binder ratios. (a) S0, (b) S0.2D0, (c) S0.2W0, (d) S0.2D0.03 and (e) S0.2D0.03.

4.8. Pore structure

Fig. 11 shows the differential pore size distribution of mortar cured for 28 days. The main peak of the pore size in S0 falls in the range of 0.1–1 μm, representing the capillary pores in the samples. The pores smaller than 0.01 μm belong to gel pores. Capillary pores larger than 10 μm are rare in S0, indicating a dense pore structure of the sample, as consistent with the results shown in Fig. 10 (a). It can be seen that the incorporation of SAP reduces the characteristic size of the capillary pores in AAS mortar, regardless of the liquid-binder ratio. This is evidence that internal curing contributes to a denser capillary porosity of the matrix. Meanwhile, more gel pores were detected in the SAP-containing mixtures, indicating the formation of more gels. These results confirm that the introduction of SAP enables a further reaction of slag and explain the higher strength of SAP-containing mixture than the reference. Besides, pores larger than 10–100 μm are identified in SAP-containing samples, which are due to the presence of SAP particles. It should be noted that the real size of the pores occupied by SAP can be larger than 100 μm, as shown in Fig. 10, but due to the inkbottle effect, the real size of these pores cannot be obtained by MIP.

The total porosity of the mixtures is shown in Fig. 12. It can be seen that the porosity of S0.2D0 and S0.2W0 is lower than that of S0. This confirms that the incorporation of SAP can facilitate the further reaction of the matrix. When SAP is added without extra water, despite the mixing way, the initial liquid-binder ratio is the same as the reference, just the distribution of liquid is different. Part of the liquid is stored in SAP and the rest exists in the interstitial space. Therefore, the initial porosity of S0.2D0 and S0.2W0 should be the
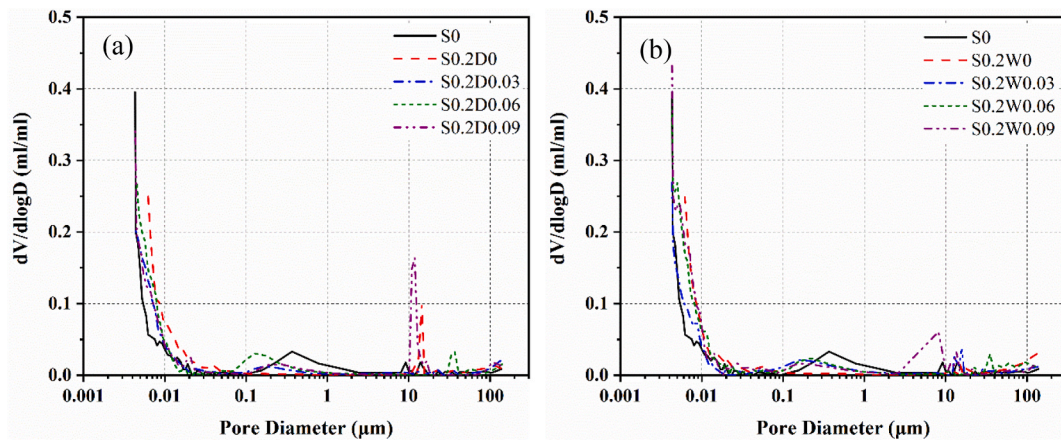
Fig. 11. Pore size distribution of AAS mortar with SAP with different liquid-binder ratios: (a) Dry mixing, (b) Wet mixing.
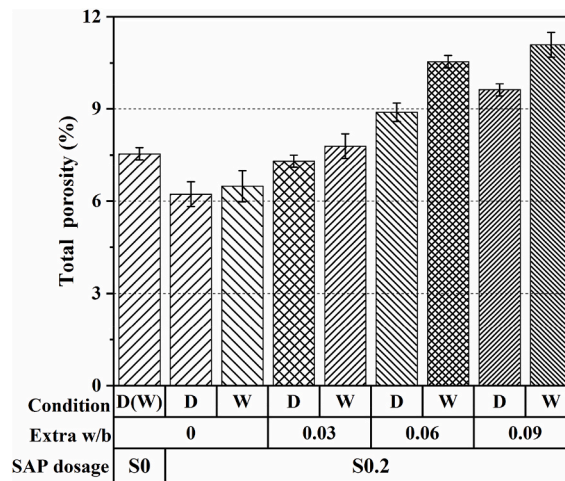

Fig. 12. Porosity of AAS mortar with SAP with different liquid-binder ratios.

same as S0. At the age of 28 days, by contrast, S0.2D0 and S0.2W0 show a finer matrix (Fig. 11) and a lower total porosity (Fig. 12), indicating that the reaction degree of the matrix is improved. This explains why S0.2D0 and S0.2W0 show higher compressive strength than the reference (Fig. 7).

With the increase of liquid-binder ratio, the porosity of the mixture increases. The larger porosity of the mixtures with extra liquid-binder ratios of 0.06 and 0.09 than that of the reference may be considered as contradictory with their higher compressive strength (see Fig. 7) of these mixtures. However, this is not true since the compressive strength is dependent on not only the porosity but also pore distribution. When SAP is present, large voids are introduced but the capillary pore space is refined and more gel pores form due to the enhanced reaction. Moreover, the voids originated from SAP are mostly isolated (see Fig. 10), having less detrimental effect on strength than connected pores with the same porosity. Hence, it is not surprising that SAP-containing mixtures with extra liquid can show larger total porosity but higher compressive strength than the reference.

Fig. 12 also shows that wet mixed samples have larger porosity than dry mixed ones with the same liquid-binder ratio, verifying again that wet mixing enables a larger absorption of SAP.

5. Conclusions

This paper studies the influence of liquid-binder ratio on the properties of SAP-containing AAS mortar. The SAP was introduced in two different sequences. The flowability, strength and autogenous shrinkage of the systems were studied. The conclusions can be drawn as follows:

(1) SAP absorbs much less in supernatant of AAS than in water, due to the high concentrations of ions in the supernatant. Mixing SAP with liquid first induces a larger absorption capacity of the SAP than mixing it with solid first.

(2) The incorporation of SAP reduces the setting time and flowability of AAS mortar if no extra liquid is added. With the increase of liquid-binder ratio, the setting time is prolonged and the flowability is improved, but the compress strength is reduced. Besides, dry mixed samples show longer setting times than wet mixed ones, while the flowability and strength are opposite. Nonetheless, the strength of internally cured AAS is higher than that of the reference even when an extra liquid-binder ratio of 0.09 is applied.

(3) The autogenous shrinkage of AAS paste can be significantly mitigated by internal curing, but the further mitigating effect by increasing the liquid-binder ratio is minor. Under the same conditions, the shrinkage mitigating effect in wet mixed samples is greater than that of dry mixed ones.

(4) The incorporation of SAP brings large isolated voids into the matrix but can refine the capillary and gel pores in the vicinity due to the enhanced reaction by internal curing. This explains the higher compressive strength of SAP-containing mixtures. Wet mixing of SAP and increasing the liquid-binder ratio both result in a larger porosity of the mixture.

CRediT authorship contribution statement

Zhengxian Yang: Conceptualization, Methodology, Supervision, Funding acquisition, Writing – review & editing. **Peng Shi:** Investigation, Writing – original draft. **Yong Zhang:** Investigation, Methodology. **Zhenming Li:** Methodology, Writing – original draft, Writing – review & editing.

Declaration of competing interest

The authors declare that they have no known competing financial interests or personal relationships that could have appeared to influence the work reported in this paper.

Acknowledgements

References

[1] C. Shi, A.F. Jiménez, A. Palomo, New cements for the 21st century: the pursuit of an alternative to Portland cement, Cement Concr. Res. 41 (2011) 750–763.

[2] B. Rajini, A.V.N. Rao, Mechanical properties of geopolymer concrete with fly ash and GGBS as source materials, Int. J. Innovat. Res. Sci. Eng. Technol. (2014) 15944–15953, 03(09.

[3] R.J. Thomas, H. Ye, A. Radlinska, et al., Alkali-activated slag cement concrete, Concr. Int. 38 (2016) 33–38, 01.

[4] L. Barcelo, J. Kline, G. Walenta, et al., Cement and carbon emissions, Mater. Struct. 47 (6) (2014) 1055–1065.

[5] J.L. Provis, Alkali-activated materials, Cement Concr. Res. 114 (2018) 40–48.

[6] T. Bakharev, J.G. Sanjayan, Y.B. Chen, Resistance of alkali-activated slag concrete to acid attack, Cement Concr. Res. 33 (10) (2003) 1607–1611.

[7] S.D. Wang, K.L. Scrivener, P.L. Pratt, Factors affecting the strength of alkali-activated slag, Cement Concr. Res. 24 (6) (1994) 1033–1043.

[8] A.R. Brough, A. Atkinson, Sodium silicate-based, alkali-activated slag mortars: part I. Strength, hydration and microstructure, Cement Concr. Res. 32 (6) (2002) 865–879.

[9] F. Collins, J.G. Sanjayan, Effect of pore size distribution on drying shrinking of alkali-activated slag concrete, Cement Concr. Res. 30 (9) (2000) 1401–1406.

[10] M. Nedeljković, Z. Li, G. Ye, Setting, strength, and autogenous shrinkage of alkali-activated fly ash and slag pastes: effect of slag content, Materials 11 (11) (2018) 2121.

[11] A.A.M. Neto, M.A. Cincotto, W. Repette, Drying and autogenous shrinkage of pastes and mortars with activated slag cement, Cement Concr. Res. 38 (4) (2008) 565–574.

[12] Z. Li, S. Zhang, X. Liang, G. Ye, Cracking potential of alkali-activated slag and fly ash concrete subjected to restrained autogenous shrinkage, Cem. Concr. Compos. 114 (2020), 103767, https://doi.org/10.1016/j.cemconcomp.2020.103767.

[13] Z. Li, M. Nedeljković, B. Chen, G. Ye, Mitigating the autogenous shrinkage of alkali-activated slag by metakaolin, Cem. Concr. Res. 122 (2019) 30–41, https://doi.org/10.1016/j.cemconres.2019.04.016.

[14] D. Snoeck, B. Moerkerke, A. Mignon, et al., In-situ crosslinking of superabsorbent polymers as external curing layer compared to internal curing to mitigate plastic shrinkage, Construct. Build. Mater. 262 (4) (2020) 120819.

[15] O.M. Jensen, P. Lura, Techniques and materials for internal water curing of concrete, Mater. Struct. 39 (9) (2006) 817–825.

[16] O.M. Jensen, P.F. Hansen, Autogenous deformation and RH-change in perspective, Cement Concr. Res. 31 (12) (2001) 1859–1865.

[17] S. Oh, Y.C. Choi, Superabsorbent polymers as internal curing agents in alkali activated slag mortars, Construct. Build. Mater. 159 (JAN.20) (2018) 1–8.

[18] W. Tu, Y. Zhu, G. Fang, et al., Internal curing of alkali-activated fly ash-slag pastes using superabsorbent polymer, Cement Concr. Res. 116 (2019) 179–190.

[19] D. Snoeck, O.M. Jensen, N.D. Belie, The influence of superabsorbent polymers on the autogenous shrinkage properties of cement pastes with supplementary cementitious materials, Cement Concr. Res. 74 (2015) 59–67.

[20] Z. Li, M. Wyrzykowski, H. Dong, et al., Internal curing by superabsorbent polymers in alkali-activated slag, Cement Concr. Res. 135 (2020) 106123.

[21] O.M. Jensen, P.F. Hansen, Water-entrained cement-based materials: II. Experimental observations, Cement Concr. Res. 32 (6) (2002) 973–978.

[22] Z. Li, T. Lu, X. Liang, et al., Mechanisms of autogenous shrinkage of alkali-activated slag and fly ash pastes, Cement Concr. Res. 135 (2020) 106107.

[23] J.B. Yang, D. Snoeck, N.D. Belie, et al., Effect of superabsorbent polymers and expansive additives on the shrinkage of alkali-activated slag, Cement Concr. Compos. 123 (2021) 104218.

[24] V. Mechtcherine, C. Schröfl, M. Wyrzykowski, et al., Effect of superabsorbent polymers (SAP) on the freeze-thaw resistance of concrete: results of a RILEM interlaboratory study, Mater. Struct. 50 (1) (2017) 14–33.

[25] D. Snoeck, D. Schaubroeck, P. Dubruel, et al., Effect of high amounts of superabsorbent polymers and additional water on the workability, microstructure and strength of mortars with a water-to-cement ratio of 0.50, Construct. Build. Mater. 72 (dec.15) (2014) 148–157.

[26] B. Craeye, M. Geirnaert, G.D. Schutter, Super absorbing polymers as an internal curing agent for mitigation of early-age cracking of high-performance concrete bridge decks, Construct. Build. Mater. 25 (1) (2011) 1–13.

[27] D.B. Jiang, X.G. Li, Y. Lv, et al., Autogenous shrinkage and hydration property of alkali activated slag pastes containing superabsorbent polymer, Cement Concr. Res. 149 (2021) 106581.

[28] A.J. Klemm, K.S. Sikora, The effect of Superabsorbent Polymers (SAP) on microstructure and mechanical properties of fly ash cementitious mortars, Construct. Build. Mater. 49 (2013) 134–143.

[29] L. Senff, R.C.E. Modolo, G. Ascensão, et al., Development of mortars containing superabsorbent polymer, Construct. Build. Mater. 95 (2015) 575–584.

[30] F. Liu, G. Zhang, T. Luo, et al., Study on pore development and water migration regularity in the process of strength formation of hydraulic concrete, Measurement (4) (2021) 109811.

[31] S.R. Zhang, K.L. Cao, C. Wang, et al., Influence of the porosity and pore size on the compressive and splitting strengths of cellular concrete with millimeter-size pores, Construct. Build. Mater. 235 (2020) 117508.

[32] C. Song, Y.C. Choi, S. Choi, Effect of internal curing by superabsorbent polymers-Internal relative humidity and autogenous shrinkage of alkali-activated slag mortars, Construct. Build. Mater. 123 (2016) 198–206.

[33] Z. Li, S. Zhang, X. Liang, et al., Internal curing of alkali-activated slag-fly ash paste with superabsorbent polymers, Construct. Build. Mater. 263 (2020) 120985, 2020.

[34] J.B. Yang, D. Snoeck, N.D. Belie, et al., Effect of superabsorbent polymers and expansive additives on the shrinkage of alkali-activated slag, Cement Concr. Compos. 123 (2021) 104218.

[35] W.X. Wu, Research on the Microstructure and Properties of Internal Curing Concrete, Wuhan University of Technology, 2010 (in Chinese).

[36] Y. Zhang, M.Z. Zhang, Transport properties in unsaturated cement-based materials - a review, Construct. Build. Mater. 72 (2014) 367–379.

[37] R.X. Lin, B. Jiang, Y.L. Huang, Study on water absorbing mechanism of absorbent resin, J. Beijing Univ. Chem. Technol. (Nat. Sci. Ed.) (1998) 22–27, 03.

[38] P. Shi, Z.X. Yang, Y. Zhang, et al., Effect of superabsorbent polymer introduction on properties of alkali-activated slag mortar, Construct. Build. Mater. (2021) (under review).

[39] C. Schröfl, D. Snoeck, V. Mechtcherine, A review of characterisation methods for superabsorbent polymer (SAP) samples to be used in cement-based construction materials: report of the Rilem TC 260-RSC, Mater. Struct. 50 (197) (2017) 1–19.

[40] C. Schröfl, V. Mechtcherine, M. Gorges, Relation between the molecular structure and the efficiency of superabsorbent polymers (SAP) as concrete admixture to mitigate autogenous shrinkage, Cement Concr. Res. 42 (6) (2012) 865–873.

[41] O.M. Jensen, Water absorption of superabsorbent polymers in a cementitious environment, in: International RILEM Conference on Advances in Construction Materials through Science and Engineering, 2011, pp. 22–35.

[42] ASTM C191-13, Standard Test Method for Time of Setting of Hydraulic Cement by Vicat Needle, ASTM International, 2013.

[43] ASTM C1437-01, Standard Test Method for Flow of Hydraulic Cement Morta, 2001. West Conshohocken, PA.

[44] GB/T 2419-2005, Test Method for Fluidity of Cement Mortar, Standards Press of China, Beijing, 2005 (in Chinese).

[45] Astm C1698-09, Standard Test Methods for Autogenous Strain of Cement Paste and Mortar, ASTM International, West Conshohocken, PA, 2014.

[46] J.M. Smith, H.C. Vanness, Introudction to Chemical Engineering Thermodynamics, 4thed., Mc- Graw-Hill, New York, 1987.

[47] O.M. Jensen, P.F. Hansen, Water-entrained cement-based materials I. Principles and theoretical background, Cement Concr. Res. 31 (2001) 647–654.

[48] S. Mönnig, Superabsorbing Additions in Concrete-Applications, Modeling and Comparison of Different Internal Water Sources, Stuttgart University, 2009.

[49] J.Y. Sun, X. Gu, Study on hydration mechanism of slag activated by alkaline, Adv. Mater. Res. 374–377 (2012) 1582–1588.

[50] H.X.D. Lee, H.S. Wong, N.R. Buenfeld, Effect of alkalinity and calcium concentration of pore solution on the swelling and ionic exchange of superabsorbent polymers in cement paste, Cement Concr. Compos. 88 (2018) 150–164.

[51] F. Puertas, A.F. Jiménez, M.T.B. Varela, Pore solution in alkali-activated slag cement pastes. Relation to the composition and structure of calcium silicate hydrate, Cement Concr. Res. 34 (2004) 139–148.

[52] S.A. Bernal, J.L. Provis, B. Walkley, et al., Gel nanostructure in alkali-activated binders based on slag and fly ash, and effects of accelerated carbonation, Cement Concr. Res. 53 (2013) 127–144.